Interaction and Multiscale Mechanics, Vol. 3, No. 4 (2010) 405-414
DOI: http://dx.doi.org/10.12989/imm.2010.3.4.405

Performance evaluation of steel and composite bridge safety barriers by vehicle crash simulation

Huu-Tai Thai*

Department of Civil and Environmental Engineering, Sejong University,
98 Kunja Dong, Kwangjin Ku, Seoul 143-747, Republic of Korea

(Received October 5, 2010, Accepted November 5, 2010)

Abstract. The performance of full-scale steel and composite bridge safety barriers under vehicle crash is evaluated by using the nonlinear explicit finite element code LS-DYNA. Two types of vehicles used in this study are passenger car and truck, and the performance criteria considered include structural strength and deformation, occupant protection, and post-crash vehicle behavior. It can be concluded that the composite safety barrier satisfies all performance criteria of vehicle crash. Although the steel safety barrier satisfies the performance criteria of occupant protection and post-crash vehicle behavior, it fails to satisfy the performance criterion of deformation. In all performance evaluations, the composite safety barrier exhibits a superior performance in comparing with the steel safety barrier.

Keywords: safety barrier; vehicle crash simulation; finite element modeling; performance evaluation.

1. Introduction

The bridge safety barrier must have the strength and the ability to absorb impact energy and prevent failure under vehicle impact. The concrete safety barrier demonstrates an excellent fall-prevention performance, but its ability of absorbing impact energy is rather poor. Meanwhile, the aluminum safety barrier is good at absorbing impact energy, but its fall-prevention performance is not ideal. Therefore, the steel and composite safety barrier, which satisfies the requirements of both fall-prevention performance and ability of absorbing impact energy, has been proposed and developed.

Reid and Sicking (1998) and Coon and Reid (2006) investigated the energy absorption of steel guardrails under impact of vehicle by using both finite element analysis and vehicle crash test. In their researches, the thin steel sheets are attached to the guardrail to dissipate drastically impact energy, and hence, to reduce casualties and deformation of the guardrail. Atahan and Cansiz (2005) made a comparison between a W-beam guardrail and a thrie-beam guardrail using both vehicle crash test and finite element simulation. The W-beam guardrail is narrow and hence it can only be applied to passenger cars, while the thrie-beam guardrail, which is wider than the W-beam guardrail, can be applied to a variety of vehicles. However, the thrie-beam guardrail is not economic due to its

* Corresponding author, Post-doctoral Fellow, E-mail: taispkt@yahoo.com

large dimension. Davids *et al.* (2006) performed a comparison study on steel bridge safety barrier and FRP-reinforced timber guardrail using bending-stress tests. Although the timber guardrail is environmentally friendly and has excellent aesthetic value, it has a larger cross section compared to steel guardrail, and hence, it is heavy and less attractive. To reduce the size of cross section and improve economic value, the authors proposed a timber guardrail reinforced with FRP. Compared to the steel guardrail, the FRP timber guardrail has higher strength performance. However, its joints can be easily broken apart and it has a larger size of cross section, and hence, it is not economic. Ren and Vesenjak (2005) described the computational analysis and experimental crash tests of a new road safety barrier. They developed and evaluated a full-scale computational model of the road safety barrier for use in crash simulations and compared the results with real crash test data. The test shows that the new safety barrier assures controllable crash energy absorption and increases the safety of vehicle occupants.

The aim of this study is to evaluate the performance of bridge safety barriers by using computer simulation. Both steel and composite bridge safety barriers are simulated to evaluate their performances under the impact of vehicles. Two types of vehicle used in this study are passenger car and truck. The dynamic performance criteria considered in this study include structural strength and deformation, occupant protection, and post-crash vehicle behavior. The nonlinear explicit dynamic code LS-DYNA is adopted to simulate the impact of vehicles on the bridge safety barriers.

2. Finite element modeling

The computational model for safety barrier crash test simulations consists of the barrier model and the vehicle model. The barrier model is established based on their design, while the vehicle model is retrieved from public accessible vehicle libraries, like the National Crash Analysis Center (2007).

2.1 Modeling of bridge safety barriers

The SB5 grade steel bridge safety barrier is chosen for this study because of its wide use in roads and highways. This model consists of columns, ribs, anchors, a concrete curb, upper, middle, and lower beams, and an impact absorbing member, as shown in Fig. 1(a). The thicknesses of the post and the impact absorbing members are 8 mm and 3.2 mm, respectively. The thickness of the upper and lower beams is 4 mm, while that of the middle beam is 8 mm. The barrier length is selected as 30 m which is identical with the barrier length in an actual crash test. The shape and thickness of the composite safety barrier are the same as those of steel safety barrier.

To prevent hourglass, full-integration shell elements with 8 integration points through thickness are used to model the columns, ribs, upper, middle, and lower beams, and impact absorbing members. The anchors and concrete curb are modeled as solid elements. The total number of element used in the modeling of safety barrier is 32,476 elements. The finite element modeling of the cross section is shown in Fig. 1(b), while the full 3D modeling of the safety barrier is shown in Fig. 2. The material properties of the steel and composite safety barriers are given in Table 1 and Table 2, respectively. In the composite safety barrier, the configuration of composite laminate is designed as 8 laminas with the fiber architecture as shown in Table 3.

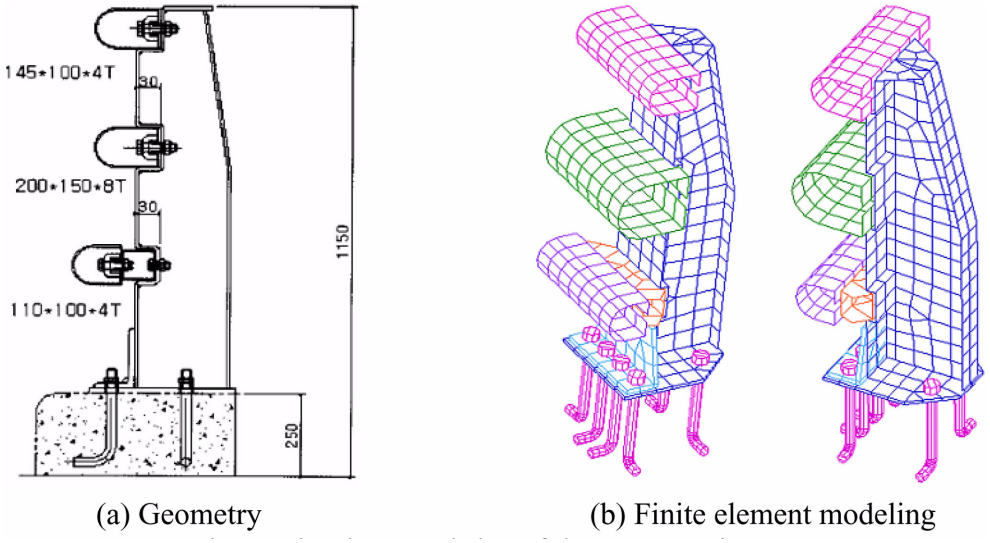

Fig. 1 The shape and size of the cross section

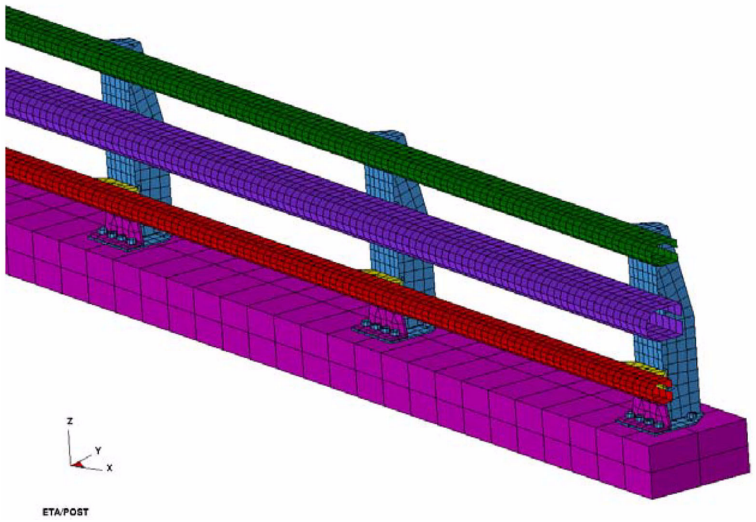

Fig. 2 Finite element modeling of bridge safety barrier

Table 1 Material properties of the steel safety barrier

Properties	Unit	Lower, middle, and upper beams
Mass of density	t/m^3	7.85
Young modulus	GPa	210.0
Poisson's ratio		0.3
Yield stress	MPa	245.0

Table 2 Material properties of the composite safety barrier

Properties	Unit	Lamina			
		Surmat #150	CSM #450	Roving #4400	DBT #600
Mass of density	t/m^3	2.62	2.62	2.62	2.62
Young modulus (E_1)	MPa	28,619	28,619	53,400	53,400
Young modulus (E_2)	MPa	28,619	28,619	14,100	14,100
Poisson's ratio (v_{12})		0.275	0.275	0.264	0.264
Tensile strength in *x*-dir.	MPa	314.1	314.1	586.0	586.0
Compressive strength in *x*-dir.	MPa	621.7	621.7	1160.0	1160.0
Tensile strength in *y*-dir.	MPa	314.1	314.1	106.0	106.0
Compressive strength in *y*-dir.	MPa	621.7	621.7	37.3	37.3

Table 3 Fiber architecture of the composite safety barrier

Layer	Lamina	Configuration	Thickness (mm)	
			Lower and upper beam	Middle beam
1	Surmat #150		0.0701	0.1402
2	CSM #450		0.21035	0.4207
3	Roving #4400		0.9827	1.9654
4	DBT #600		0.28055	0.5611
5	Roving #4400		0.9827	1.9654
6	DBT #600		0.28055	0.5611
7	Roving #4400		0.9827	1.9654
8	CSM #450		0.21035	0.4207

2.2 Modeling of vehicles

Finite element modeling of a 1.3-ton passenger car (Ford Taurus) and an 8-ton truck (Ford single unit truck) is taken from the National Crash Analysis Center (2007) as shown in Fig. 3. The total numbers of elements for passenger car and truck are 28,578 and 20,727, respectively. To fulfill the weight standard regulations, the mass of the 8-ton truck is increased to 14 tons to adapt the required values.

2.3 Boundary condition and contact description

The fixed boundary conditions are applied to the anchor, the bottom of concrete curb, and the road. The AUTOMATIC-SURFACE-TO-SURFACE contact condition is assigned to the contact between the vehicle and the bridge safety barrier. The static and dynamic friction coefficients of the contact between vehicle and safety barrier are given in Table 4 (Avallone *et al*. 2006).

2.4 Crash conditions

Based on the standard regulations (MLTM 2001), the initial velocities of the passenger car and the

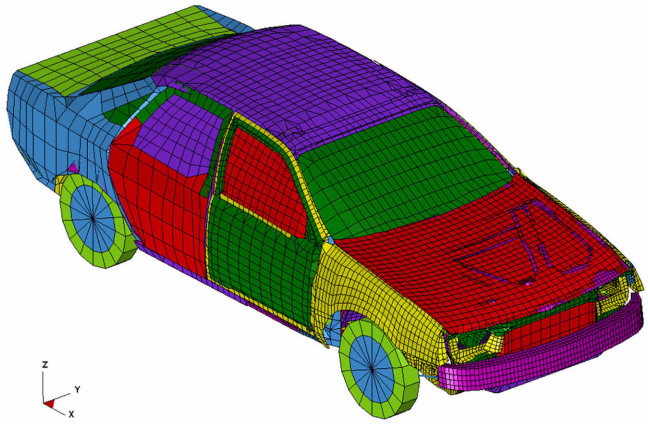

(a) Passenger car

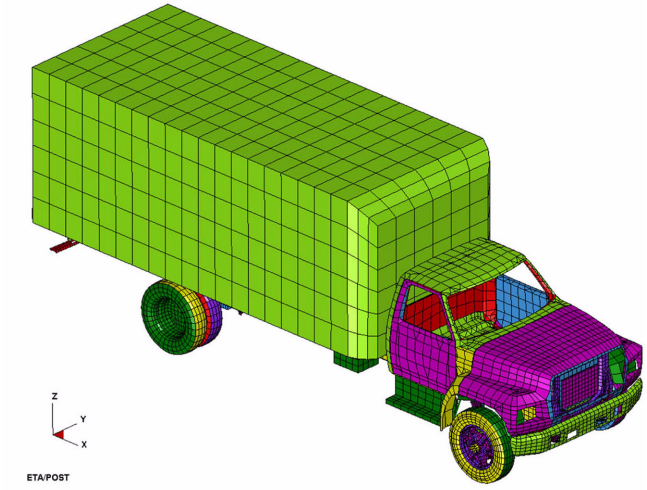

(b) Truck

Fig. 3 Three-dimensional modeling of vehicles

Table 4 Friction coefficients of the contact between vehicle and safety barrier

Safety barrier	Passenger car		Truck	
	Static	Dynamic	Static	Dynamic
Steel barrier	0.20	0.16	0.13	0.12
Composite barrier	0.50	0.40	0.20	0.16

truck are 100 km/h and 80 km/h, respectively. The impact angles between vehicle and safety barrier are 15° and 20° for the passenger car and the truck, respectively.

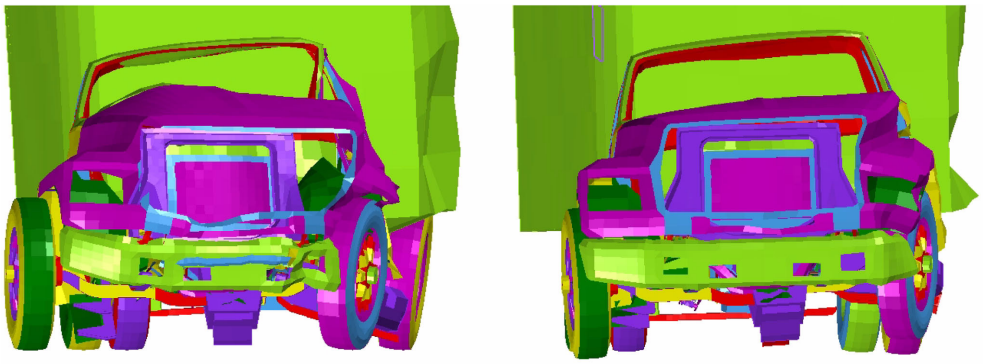

(a) The steel bridge safety barrier (b) The composite bridge safety barrier

Fig. 4 Comparison of deformation shape of the truck

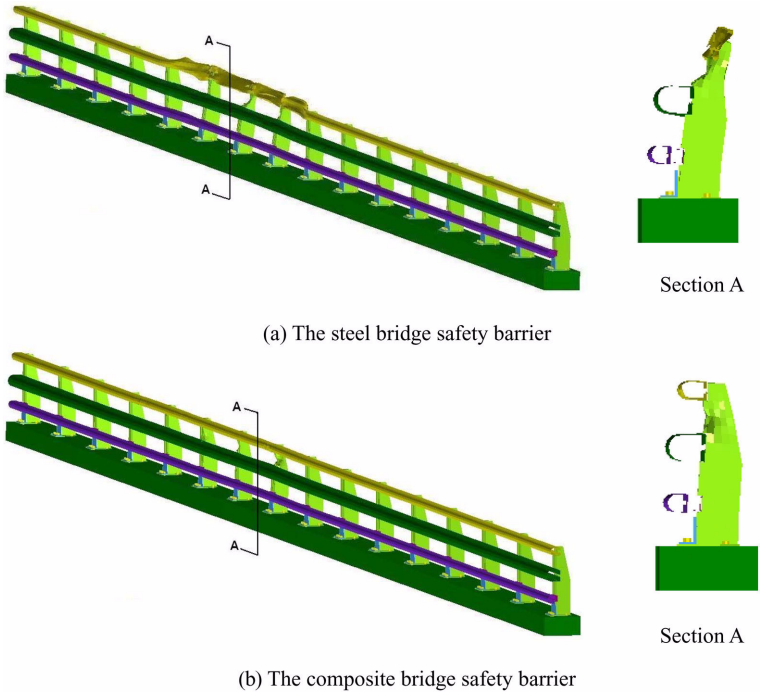

(a) The steel bridge safety barrier

(b) The composite bridge safety barrier

Fig. 5 Comparison of deformation shape of bridge safety barrier

3. Crash simulation results

3.1 Structural strength performance

Since the weight and impact angle of the passenger car are smaller than those of the truck, the evaluations of structural strength performance are often carried out on the truck. Fig. 4 shows the

Table 5 Deformation of bridge safety barrier

Performance item	Criteria	Steel barrier	Composite barrier	Composite/Steel
Maximum deformation (m)	≤ 0.3	0.376	0.064	0.17
Impact energy (kJ)	≥ 230	232.9	232.9	1.00

Table 6 Comparison of occupant protection performance

Occupant protection performance item	Criteria	Steel barrier	Composite barrier	Composite/Steel
THIV (m/s)	≤ 9	7.7	4.3	0.56
PHD (g), g = 9.81 m/s^2	≤ 20	17.9	14.6	0.82

comparison of deformation of the truck impacting on the steel and composite barriers. It can be observed that the deformation of the truck mainly occurred in the front bumper. The maximum distortions of the truck impacting on the steel and composite barriers are 25.9 cm and 21.4 cm, respectively, which indicates that the composite safety can reduce the deformation of the vehicle by 17.4% in comparing with the steel barrier.

The deformation configurations of the steel and composite safety barriers under the truck impact are compared in Fig. 5. The maximum displacements of the steel barrier at the lower, middle, and upper beams are 376.4 mm, 56.2 mm, and 16.5 mm, respectively, while those of the composite barrier are 64 mm, 31.3 mm, and 8.14 mm, respectively. It can be seen that the composite barrier has superior strength in comparing with the steel barrier.

The comparison of the strength performance of the steel and composite safety barriers under the impact of the truck is presented in Table 5. It can be observed that the steel safety barrier fails to satisfy the criterion value of the strength performance, whereas the composite safety barrier satisfies the strength performance.

3.2 Occupant protection performance

Since the weight of passenger car is much smaller than that of truck, the capability of occupant protection of the car under impact is lower than that of the truck. Therefore, the occupant protection performance is only evaluated for the passenger car. Two parameters, THIV (Theoretical Head Impact Velocity) and PHD (Post-impact Head Deceleration) (Ross *et al*. 1993), are used to evaluate the occupant protection. THIV indicates an occupant's impact risk level when a vehicle impacts into barrier. It refers to the velocity at which the driver's head moves until it strikes a surface within the interior of the vehicle. The magnitude of the velocity of the theoretical head impact is considered to be a measure of impact severity. PHD refers to the acceleration of the head when the occupant strikes the vehicle interior due to secondary impact caused by the primary impact. The head is presumed to remain in contact with the surface during the remaining impact period. The values of THIV and PHD are determined for the passenger car as presented in Table 6. It can be observed that both steel and composite safety barriers used in this study satisfied the criterion values of occupant protection performance, and the composite safety barrier has superior occupant protection performance to the steel safety barrier.

Table 7 Comparison of the post-crash vehicle behavior

Post-crash performance	Criteria	Steel barrier	Composite barrier	Composite/Steel
Departure velocity/ impact velocity	≥ 0.6	Car: 0.69 Truck: 0.76	Car: 0.71 Truck: 0.82	Car: 1.03 Truck: 1.08
Departure angle/ impact angle	≤ 0.6	Car: 0.20 Truck: 0.39	Car: 0.19 Truck: 0.25	Car: 0.95 Truck: 0.64

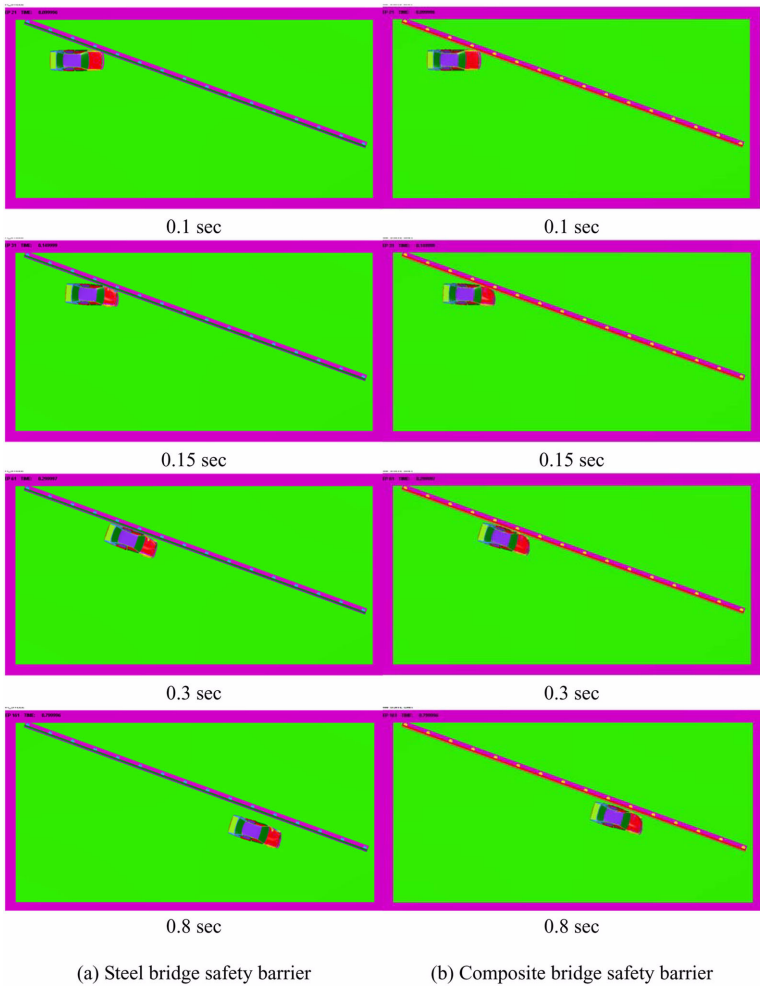

Fig. 6 Crash simulation of passenger car

3.3 Post-crash vehicle behavior

Two criteria are used to evaluate the post-crash behavior of vehicle: (1) the change of departure velocity in comparing with the impact velocity; and (2) the change of departure angle in comparing with the impact angle. In order to satisfy the performance criteria, the departure velocity should be

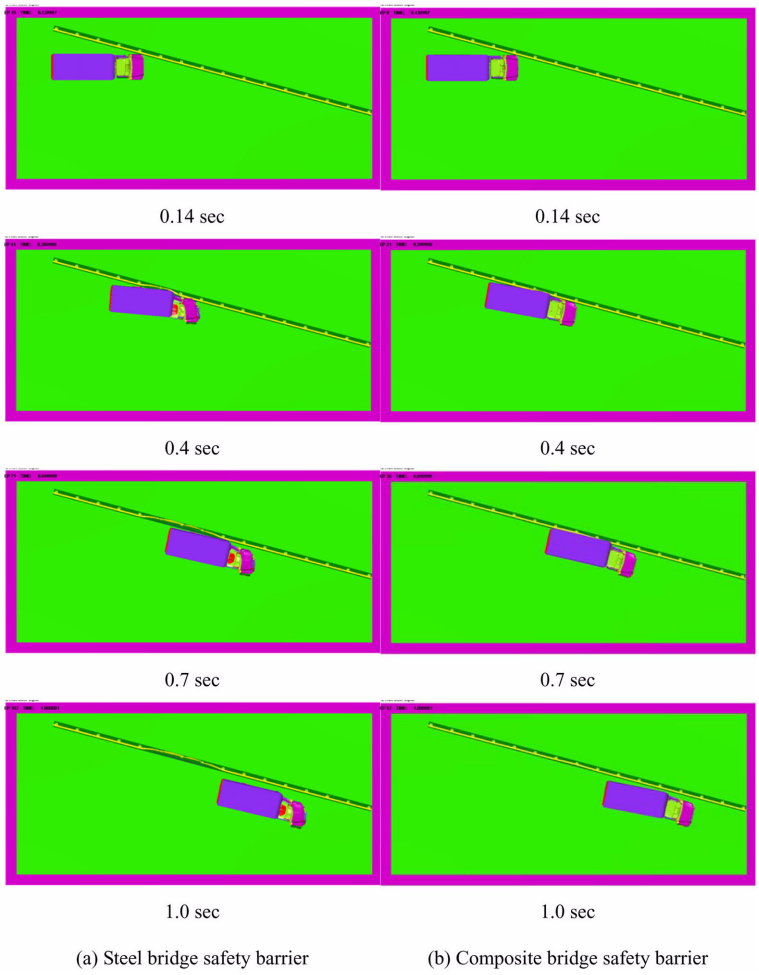

Fig. 7 Crash simulation of truck

higher than 60% of the impact velocity, and the departure angle should be lower than 60% of the impact angle. The comparison of the performance of post-crash behavior of vehicles is shown in Table 7. It can be seen that both steel and composite bridge safety barriers used in this study satisfied the performance criteria of post-crash vehicle, and the composite safety barrier has a superior post-crash performance in comparing with the steel safety barrier. The crash simulations of the passenger car and the truck are illustrated in Fig. 6 and Fig. 7, respectively.

4. Conclusions

Computational nonlinear explicit dynamic analysis is employed for evaluation on the performance of the bridge safety barriers under vehicle crash. The performance of two types of steel and composite safety barriers under the crash of passenger car and truck are evaluated and compared

with the performance criteria. The composite safety barrier satisfies all performance criteria of vehicle crash such as the deformation, the occupant protection, and the post-crash vehicle behavior. Although the steel safety barrier satisfies the performance criteria of occupant protection and post-crash vehicle behavior, it fails to satisfy the deformation performance. In all performance evaluations, the composite safety barrier exhibits a superior performance in comparing with the steel safety barrier.

Acknowledgements

This research was supported by Korea Ministry of Land, Transport and Maritime Affairs through grant B01 of Construction Technology Innovation Program.

References

Atahan, A.O. and Cansiz, O.F. (2005), "Impact analysis of a vertical flared back bridge rail-to-guardrail transition structure using simulation", *Finite Elem. Anal. Des.*, **41**(4), 371-396.

Avallone, E., Baumeister, T. and Sadegh, A. (2006), *Marks' standard handbook for mechanical engineering*, McGrew-Hill, NY.

Coon, B.A. and Reid, J.D. (2006), "Reconstruction techniques for energy-absorbing guardrail end terminals", *Accident Anal. Prevent.*, **38**(1), 1-13.

Davids, W.G., Botting, J.K. and Peterson, M. (2006), "Development and structural testing of a composite-reinforced timber highway guardrail", *Constr. Build. Mater.*, **20**(9), 733-743.

FHWA/NHTSA (2007), "National crash analysis center", *Finite Element Model Archive: Available online: http://www.ncac.gwu.edu/vml/models.html*.

MLTM (2001), *Vehicle protection security facility actual crash test handbook*, Korea Ministry of Land, Transport and Maritime Affairs.

Reid, J.D. and Sicking, D.L. (1998), "Design and simulation of a sequential kinking guardrail terminal", *Int. J. Impact Eng.*, **21**(9), 761-772.

Ren, Z. and Vesenjak, M. (2005), "Computational and experimental crash analysis of the road safety barrier", *Eng. Fail. Anal.*, **12**(6), 963-973.

Ross, H.E., Jr., Sicking, D.L., Zimmer, R.A., and Michie, J.D. (1993), "Recommended procedures for the safety performance evaluation of highway features", Transportation Research Board, NCHRP Report 350.